electronics

MDPI

Article

A Secure Cooperative Transmission of Image Super-Resolution in Wireless Relay Networks

Hien-Thuan Duong [1,†], Ca V. Phan [1,*], Quoc-Tuan Vien [2] and Tuan T. Nguyen [3]

[1] Faculty of Electrical and Electronics Engineering, Ho Chi Minh City University of Technology and Education, Ho Chi Minh City 700000, Vietnam; thuandh.ncs@hcmute.edu.vn
[2] Faculty of Science and Technology, Middlesex University, London NW4 4BT, UK; q.vien@mdx.ac.uk
[3] School of Computing and Mathematical Sciences, University of Greenwich, London SE10 9LS, UK; tuan.nguyen@greenwich.ac.uk
* Correspondence: capv@hcmute.edu.vn
† Current address: Faculty of Electronics and Telecommunications, Sai Gon University, Ho Chi Minh City 700000, Vietnam.

Abstract: The image transmission over wireless media experiences not only unavailable performance loss caused by the environment and hardware issues, but also information leakage to eavesdroppers who can overhear and attempt to recover the images. This paper proposes a secure cooperative relaying (SCR) protocol for the image communications in wireless relay networks (WRNs) where Alice sends high-resolution (HR) images to Bob with the assistance of a relaying user named Relay, and in the presence of an eavesdropper named Eve. In order to enhance the security of the image communications, random linear network coding (RLNC) is employed at both Alice and Relay to conceal the original images from Eve with RLNC coefficient matrices and reference images in the shared image datastore. Furthermore, the original HR images are downscaled at Alice to save transmission bandwidth and image super-resolution (ISR) is adopted at Bob due to its capability to recover the HR images from their low-resolution (LR) version, while still maintaining the image quality. In the proposed SCR protocol, Bob can decode both the original images transmitted from Alice over the direct link and the images forwarded by Relay over the relaying links. Simulation results show that the SCR protocol achieves a considerably higher performance at Bob than at Eve since Eve does not know the coefficient matrices and reference images used at Alice and Relay for the RLNC. The SCR protocol is also shown to outperform the counterpart secure direct transmission protocol without the relaying links and secure relaying transmission without the direct link. Additionally, an increased scaling factor can save the transmission bandwidth for a slight change in the image quality. Moreover, the impacts of direct, relaying and wiretap links are evaluated, verifying the effectiveness of the SCR protocol with the employment of Relay to assist the image communications between Alice and Bob in the WRNs.

Keywords: image communication; deep learning; image super-resolution; random linear network coding; cooperative communications; wireless relay networks

Citation: Duong, H.-T.; Phan, C.V.; Vien, Q.-T.; Nguyen, T.T. A Secure Cooperative Transmission of Image Super-Resolution in Wireless Relay Networks. *Electronics* **2023**, *12*, 3764. https://doi.org/10.3390/electronics12183764

Academic Editor: Ashwin Ashok

Received: 13 July 2023
Revised: 27 August 2023
Accepted: 30 August 2023
Published: 6 September 2023

1. Introduction

Cooperative wireless communications have attracted growing interest with emerging technologies for data transmission with higher reliability and security. By leveraging a shared wireless medium, communication between two end users can be achieved collaboratively with the help of intermediary users, also known as a relay nodes [1]. The cooperative communication techniques have been adopted in various wireless network models where the relay nodes can be used to not only extend network coverage with enhanced system throughput, but also improve signal quality with higher spatial diversity gains [2].

Over relay networks, relay nodes do not simply store the data received from source nodes, but they can process the data prior to forwarding them to destination nodes. Specif-

ically, the network coding (NC) concept, which was originally proposed in [3], has been applied at the relay nodes to improve the throughput of wireless relay networks [4,5]. The incoming data packets from the source nodes can be subjected to random linear NC (RLNC) operations by the relay nodes. The destination nodes can retrieve the data of the source nodes if there are enough mixed data packets and they are aware of the linear coefficients [6]. A variety of NC-based protocols have also been developed for typical relay channel models, such as relay-assisted bidirectional channels [7], broadcast channels [8] and multicast channels [9]. Additionally, RLNC can protect the communication [10] by limiting the degrees of freedom (decoding abilities) that the eavesdropper(s) receive.

Considering image communications over wireless relay networks (WRNs), the image data from a source node can be delivered to a destination node either directly or after two hops through a relay node (for example, source-to-relay and relay-to-destination links). Inspired by the benefit of cooperative diversity, a cooperative communication method exploiting both relaying and direct links is considered in this work to enhance the performance of the image communications in the WRNs. Although RLNC and traditional relaying protocols can be used for image communication, there are a number of data privacy and transmission bandwidth concerns that need to be taken into consideration. In this research, we present a secure cooperative communication protocol that is inspired by image super-resolution (ISR) and RLNC in order to not only hide the picture but also reduce the bandwidth used for image communications in WRNs. The following is a summary of the paper's main contributions:

- With the aid of a relaying user, a secure cooperative relaying (SCR) protocol is proposed for image communications between Alice and Bob in WRNs. The original high-resolution (HR) photograph at Alice is first downscaled using the suggested technique in order to conserve transmission bandwidth. Prior to being sent to both the relaying user and Bob, this low-resolution (LR) image that has been downscaled is mixed with a reference image using RLNC encoding to hide the actual image from Eve, a potential spy. The received image is decoded, combined with RLNC, and sent to Bob at the relaying user. Bob can decode and recover the original HR image [11] from both Alice and the relay by using RLNC decoding and ISR. The novel feature of the proposed approach is *how it effectively integrates and ties the advantages of the RLNC and ISR into a single framework for image communications in WRNs with limited transmission bandwidth*.
- The proposed SCR protocol's effectiveness is assessed and compared with that of two other schemes: *secure direct transmission (SDT), which was investigated in [12], where Alice sends the RLNC-encoded image directly to Bob without the assistance of any relaying user, and secure relaying transmission (SRT), where Alice sends the RLNC-encoded image to Bob only via a relaying user given no direct link between Alice and Bob.* The SCR protocol outperforms both the SDT and SRT systems, according to simulation results. Because both Alice and the relaying user used RLNC, it was demonstrated that Bob performed far better than Eve. It is also demonstrated that the original HR image may be downscaled to a much lower resolution image before transmission to conserve transmission bandwidth while still offering equivalent performance at various scales and far higher performance than Eve.
- It is demonstrated that the direct link, or the Alice–Bob link, and relaying links, or the Alice–Relay and Relay–Bob links, have significant effects on performance when taking into account the effects of communication interactions between Alice, Bob, Eve and the relaying user. It is shown that the proposed SCR system outperforms the SDT and SRT protocols. Given the high quality of the relaying links, the SRT protocol performs better than the SDT protocol, whereas the SDT protocol excels when the direct link is of greater quality than the relaying links. This demonstrates the advantage of using the relay for improved performance in the proposed SCR approach.

The rest of this paper is organised as follows: Firstly, Section 2 presents the related works as bases and motivation for our work. Section 3 describes the system model of typical image communications in a WRN with the existence of wiretap links. The proposed

SCR protocol for secure ISR over WRNs is presented in Section 4, followed by simulation results in Section 5 to validate the performance of the proposed SCR protocol and compare it with the counterpart protocols. Finally, Section 6 concludes this paper by outlining its main contributions with suggestions for future works.

2. Related Works

ISR has utilized generalization abilities of deep learning approaches to learn a mapping between the LR and HR images in order to produce an HR image from an LR version [11,13,14]. Multiple ISR architectures following this approach, have been developed, such as super-resolution convolutional neural network [15], Laplacian pyramid SR [16], deep back-projection networks [17], super-resolution feedBack networks [18], very deep super resolution (VDSR) [19] and deep residual network [20]. In an effort to improve performance, a deep learning (DL)-based aggregation has been deployed, such as the reliability-aware neural network (RANN) [21] for signature categorization, etc. Among these methods, the VDSR was shown to reproduce an HR image from its LR versions achieving a high performance with a high running speed. Specifically, there are 64 filters in each convolutional layer along with rectified linear units in the VDSR framework. Due to its advanced architecture, the VDSR has been adopted in different areas, such as network security [22], machinery [23], seismic analysis [24] and image communications [25]. It is worth noticing that the LR images with reduced dimensions save the transmission bandwidth considerably.

Regarding to the image communications, privacy should be taken into account. Techniques for image protection fall under two approaches: information concealment and cryptography. Watermarking and steganography are two categories of information concealment methods. In cryptography, a plain image is first scrambled using a hash or an encryption algorithm, and then, at the recipient, a ciphered image is used to recover the secret image using a decryption function. To protect images with limited common information, a secure image hash-based geometric modification approach was specifically suggested in [26]. The image security can be further enhanced with transformation methods, such as scaling, shifting and rotation. Numerous encryption methods have been examined in [27]. In watermarking, digital information is inserted into a cover image. Digital information can be visible or invisible and is typically employed to protect copyright or authenticate images. In [28], to secure the telemedicine picture transmission, an optimized semi-tensor product with compressed sensing and a digital watermarking method was developed, obtaining high decodability over various environments such as white Gaussian noise, Poisson noise and impulsive noise.

Along with encryption method, there exists another method to conceal information within other non-secret data, which is well known as steganography [29,30]. Although two approaches have different techniques, they both have the same aim to protect the data from undesired users. Steganography is, however, more favorable due to its low complexity compared with encryption methods which require encryption and decryption algorithms at both ends. Stenography can be applied for hiding text, image, audio and video, among which the images with a number of redundant bits are selected as the most suitable for steganography. A simple technique employing least significant bit was proposed in [31], where the last bit of each pixel is exploited to store the data bit in the secret message. The image can be further concealed by transforming from the spatial to frequency domain with discrete cosine transform [32] and discrete wavelet transform [33]. Over different frequency bands, the image can be modified so that the change is not recognized. However, the hidden image in this technique must be smaller than the cover image, which may restrict its application. In contrast to traditional image steganography, coverless steganography embeds secret data directly into the characteristics of the cover image, such as its edge, texture, pixel brightness value and color, without any designations or alterations. There have been a number of significant contributions [34] in this area.

Considering data communications over WRNs, NC has been adopted in a number of works to improve the network throughput, e.g., in [35,36]. A form of secure NC was originally proposed in [37]. The authors in [10] demonstrated that RLNC can protect communication in a network where any intermediate nodes are susceptible to wiretapping. Originally proposed in [35], the NC implemented for the physical layer in a two-way relay wireless network can increase system throughput by 100%. Secure NC was used in [38] to improve the security of wiretap channels and in [5] for secure relaying with modify-and-forward in WRNs, where the relay randomly and linearly combines the decoded data with the encrypted key before forwarding to the destination using the RLNC approach. In order to increase security, latency and power consumption in WRNs, the authors of [39] took advantage of the benefits of RLNC and relay selection procedures. Hybrid NC, where the output of the NC is separated into two sets, one of which is transmitted freely and the other of which is processed by security covert methods based on the physical layer, has been proposed in [40] as a way to increase the security of the wireless channel.

Our work, which is inspired by these methods, proposes a secure cooperative relaying protocol over WRNs that exploits the use of the RLNC idea combined with a reference image used as coverless steganography to secure images transmitted in the network, as well as the employment of ISR to recover the original HR images at Bob from their LR versions in order to conserve transmission bandwidth at Bob and the relay.

3. System Model

With the help of a relaying user named Relay ($\mathcal{R}$) and in the presence of Eve ($\mathcal{E}$), who is attempting to eavesdrop on the photo, Alice ($\mathcal{A}$) wants to communicate a private image to Bob ($\mathcal{B}$) in a WRN. Figure 1 shows a typical secure image communication paradigm in this scenario. Since Alice and Bob are considered to have a direct link, Alice can send Bob the image with or without the aid of a Relay. Eve is expected to be in the middle of Alice and Bob, as well as close to the Relay, as illustrated in Figure 1. As a result, there are two wiretap connections from Alice and Relay to Eve which are colored red.

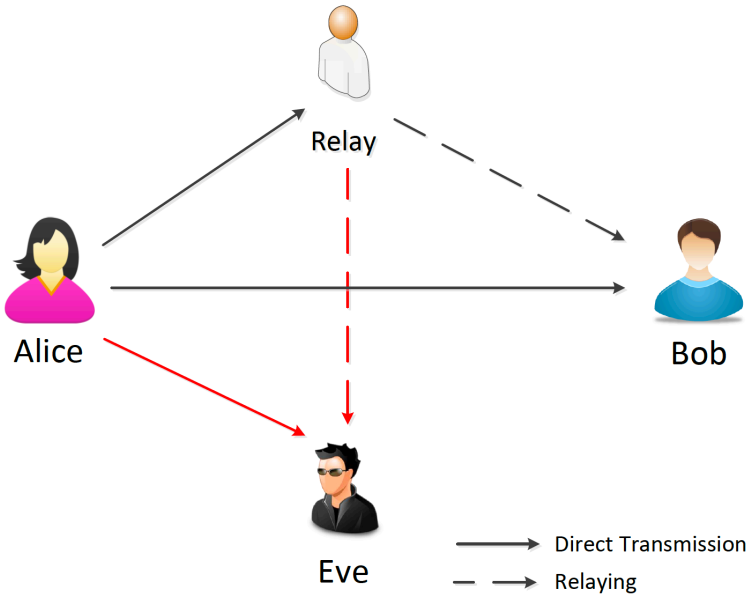

Figure 1. System model of secure image communications in a typical WRN.

It is assumed that the image transmission between nodes $\mathcal{X}$ and $\mathcal{Y}$, $\{\mathcal{X}, \mathcal{Y}\} \in \{\mathcal{A}, \mathcal{B}, \mathcal{R}, \mathcal{E}\}$, experiences additive white Gaussian noise (AWGN) at the receiver, which degrades the image. Given that Gaussian noise is frequently used to simulate the impacts of numerous random processes from natural sources that occur in digital images, it was chosen as the best fit to represent the additive noise in the unwanted signals at the receiving

node. In this work, we focus on typical three-channel, or red, green and blue, color images. Thus, an $M \times N \times 3$ array can be utilized to represent an image $\mathbf{I}$ of size $M \times N$. It is expected that Alice, Relay and Bob perfectly share channel information and decoding information via authorized channels.

In the proposed SCR protocol, the image communications between Alice and Bob can be realized in two time slots: (i) in the first time slot, Alice sends the RLNC-encoded image to both Relay and Bob; and (ii) in the second time slot, Relay decodes the received image, performs RLNC encoding and forwards the encoded image to Bob. Over the shared wireless media, Eve can overhear and try to decode the images in both time slots from Alice and Relay using the wiretap links.

4. Proposed Secure Cooperative Relaying for Image Communications

In order to improve the security of images transferred over WRNs with low transmission bandwidth, we introduce SCR protocol in this section, along with the image processing, encoding and decoding procedure.

4.1. Image Downscaling, Concealing and Transmission at Alice

To reduce transmission bandwidth use, Alice first creates an LR version of the original HR image by downscaling with bicubic interpolation (the bicubic filter is taken into consideration in this work due to its low processing complexity) and encoding it before transmission, using the same strategy as ISR [19].

Let $\mathbf{I}_{\mathcal{A}}^{(HR)}$ of size $M \times N \times 3$ denote the original RGB image that Alice wants to send to Bob. Applying bicubic interpolation with a scaling factor ϵ, we can obtain an LR version of the original image as $\mathbf{I}_{\mathcal{A}}^{(LR)}$ of size $M' \times N' \times 3$, where $M' = \lceil M/\epsilon \rceil$ and $N' = \lceil N/\epsilon \rceil$. Here, $\lceil \cdot \rceil$ denotes the ceiling operator.

In the proposed SCR protocol, RLNC is applied to encode the image at Alice by mixing the LR image, i.e., $\mathbf{I}_{\mathcal{A}}^{(LR)}$, with a reference image, denoted by $\mathbf{I}_{\mathcal{A}}^{(ref)}$, which is randomly selected from a shared image datastore $\mathfrak{S}$. The image datastore $\mathfrak{S}$ can be accessed by all legitimate users, i.e., Alice, Bob and Relay. Additionally, a Trust and Reputation Management (TRM) system [41] is used to lessen the effects of errant or misbehaving nodes in the WRN. The encoded image at Alice, denoted by $I_{\mathcal{A}}^{(enc)}$, can be given by

$$\mathbf{I}_{\mathcal{A}}^{(enc)} = \mathbf{M}_{\mathcal{A},1} \circ \mathbf{I}_{\mathcal{A}}^{(LR)} + \mathbf{M}_{\mathcal{A},2} \circ \mathbf{I}_{\mathcal{A}}^{(ref)}, \tag{1}$$

where $\mathbf{M}_{\mathcal{A},k}$, $k \in \{1, 2\}$, of size $M' \times N' \times 3$ are RLNC coefficient matrices at Alice and $\circ$ denotes the element-wise multiplication, also known as the Hadamard product, of two matrices. Let $\alpha_{\mathcal{A},m,n,p}^{(k)}$, $m \in \{1, 2, \ldots, M'\}$, $n \in \{1, 2, \ldots, N'\}$, $p \in \{1, 2, 3\}$ denote the coefficient in matrix $\mathbf{M}_{\mathcal{A},k}$. In order to restrict the value of the image pixels of the encoded image not exceeding its range, $\alpha_{\mathcal{A},m,n,p}^{(k)}$ is in the range $[0, 1]$ and $\alpha_{\mathcal{A},m,n,p}^{(1)} + \alpha_{\mathcal{A},m,n,p}^{(2)} = 1$.

Remark 1 (Impacts of RLNC coefficient matrices)**.** *Coefficients in RLNC matrices* $\mathbf{M}_{\mathcal{A},1}$ *and* $\mathbf{M}_{\mathcal{A},2}$ *represent the fractions of the LR image* $\mathbf{I}_{\mathcal{A}}^{(LR)}$ *and the reference image* $\mathbf{I}_{\mathcal{A}}^{(ref)}$*, respectively, in the encoded image at Alice. An appropriate allocation of the RLNC coefficients would enhance the image decodability, while maintaining the security of the image communications in WRNs. Specifically, a higher* $\alpha_{\mathcal{A},m,n,p}^{(1)}$, $m \in \{1, 2, \ldots, M'\}$, $n \in \{1, 2, \ldots, N'\}$, $p \in \{1, 2, 3\}$, *results in a better decodability of image pixel, while more secure image communications can be obtained with a higher* $\alpha_{\mathcal{A},m,n,p}^{(2)}$.

Remark 2 (Impacts of scaling factor)**.** *Transmission bandwidth of* ϵ^2 *is saved at Alice when the original HR image is downscaled by a scaling factor of* ϵ*. This is due to the fact that the image size is reduced* ϵ *times in both directions..*

The RLNC-encoded image $\mathbf{I}_{\mathcal{A}}^{(enc)}$ is then sent to both Relay and Bob in the form of a modulated data packet, denoted by $\mathbf{x}_{\mathcal{A}}$, over the legitimate wireless channels.

4.2. Image Decoding at Relay and Image Recovery at Bob in the First Time Slot

In the first time slot, the received signals at Relay and Bob can be written by

$$\mathbf{r}_{\mathcal{X}}^{(1)} = \mathbf{x}_{\mathcal{A}} + \mathbf{n}_{\mathcal{X}}^{(1)}, \tag{2}$$

where $\mathcal{X} \in \{\mathcal{R}, \mathcal{B}\}$ and $\mathbf{n}_{\mathcal{X}}^{(1)}$ is an independent AWGN vector at node $\mathcal{X}$ with zero mean and variance of $\sigma_{\mathcal{X},1}^2$ for each entry.

The data received from Alice are decoded by Relay and Bob indicated by $\hat{\mathbf{x}}_{\mathcal{X}}^{(1)}$, $\mathcal{X} \in \{\mathcal{R}, \mathcal{B}\}$. A deep neural network is employed to denoise the image using a pretrained DnCNN network [24]. Let $\bar{\mathbf{I}}_{\mathcal{X}}^{(1)}$ denote the denoised image at node $\mathcal{X}$. Using the shared reference image from Alice, i.e., $\mathbf{I}_{A}^{(ref)}$, and RLNC coefficient matrices, i.e., $\mathbf{M}_{\mathcal{A},1}$ and $\mathbf{M}_{\mathcal{A},2}$, Relay and Bob can decode the original image as

$$\hat{\mathbf{I}}_{\mathcal{R}}^{(1)} = \left(\bar{\mathbf{I}}_{\mathcal{R}}^{(1)} - \mathbf{M}_{\mathcal{A},2} \circ \mathbf{I}_{\mathcal{A}}^{(ref)}\right) \oslash \mathbf{M}_{\mathcal{A},1}, \tag{3}$$

$$\hat{\mathbf{I}}_{\mathcal{B}}^{(1)} = \left(\bar{\mathbf{I}}_{\mathcal{B}}^{(1)} - \mathbf{M}_{\mathcal{A},2} \circ \mathbf{I}_{\mathcal{A}}^{(ref)}\right) \oslash \mathbf{M}_{\mathcal{A},1}, \tag{4}$$

respectively, where $\oslash$ denotes the element-wise division of two matrices.

Additionally, utilizing the ISR framework, which was trained using the publicly accessible IAPR TC-12 Benchmark dataset [42], Bob recovers the full size of the original image after decoding. The hyper-parameters used for training in the proposed SCR protocol are similar to those in [19] with batch size of 64 in 100 epochs, initial learning rate of 0.1 and different scaling factors $\epsilon = \{2, 4, 6, 8, 10\}$. The upscaled HR image recovered at Bob in the first time slot, denoted by $\hat{\mathbf{I}}_{\mathcal{B}}^{(HR,1)}$, can be thus obtained by

$$\hat{\mathbf{I}}_{\mathcal{B}}^{(HR,1)} = \nabla_{\epsilon}(\hat{\mathbf{I}}_{\mathcal{B}}^{(1)}), \tag{5}$$

where $\nabla_{\epsilon}(\cdot)$ denotes the ISR operator to reconstruct the upscaled images with scaling factor ϵ.

4.3. Image Concealing and Forwarding at Relay in the Second Time Slot

In the proposed SCR protocol, Relay first conceals the recovered image from Alice prior to forwarding to Bob in the second time slot.

Following the RLNC method, Relay encodes the recovered image from Alice, i.e., $\hat{\mathbf{I}}_{\mathcal{R}}^{(1)}$, by mixing it with a reference image, denoted by $\mathbf{I}_{\mathcal{R}}^{(ref)}$. The reference image $\mathbf{I}_{\mathcal{R}}^{(ref)}$ at Relay is different from that at Alice, though it is also randomly selected from the same image datastore $\mathfrak{S}$ shared between the legitimate users. It is defined as follows:

$$\mathbf{I}_{\mathcal{R}}^{(enc)} = \mathbf{M}_{\mathcal{R},1} \circ \hat{\mathbf{I}}_{\mathcal{R}}^{(1)} + \mathbf{M}_{\mathcal{R},2} \circ \mathbf{I}_{\mathcal{R}}^{(ref)}, \tag{6}$$

where $\mathbf{M}_{\mathcal{R},k}$, $k \in \{1, 2\}$, of size $M' \times N' \times 3$ are RLNC coefficient matrices at Relay. Denoting the coefficient in matrix $\mathbf{M}_{\mathcal{R},k}$ by $\alpha_{\mathcal{R},m,n,p}^{(k)}$, $m \in \{1, 2, \ldots, M'\}$, $n \in \{1, 2, \ldots, N'\}$, $p \in \{1, 2, 3\}$, the same condition is applied to restrict the value of the image pixels of the encoded image at Relay not exceeding its range, i.e., $0 \leq \alpha_{\mathcal{R},m,n,p}^{(k)} \leq 1$ and $\alpha_{\mathcal{R},m,n,p}^{(1)} + \alpha_{\mathcal{R},m,n,p}^{(2)} = 1$.

Then, Relay forwards the encoded image $\mathbf{I}_{\mathcal{R}}^{(enc)}$ to Bob in the form of a modulated data packet, denoted by $\mathbf{x}_{\mathcal{R}}$.

4.4. Image Recovery, Super Resolution and Fusion at Bob in the Second Time Slot

The received signal at Bob in the second time slot can be written by

$$\mathbf{r}_{\mathcal{B}}^{(2)} = \mathbf{x}_{\mathcal{R}} + \mathbf{n}_{\mathcal{B}}^{(2)}, \tag{7}$$

where $\mathbf{n}_{\mathcal{B}}^{(2)}$ is an AWGN vector at Bob with zero mean and variance of $\sigma_{\mathcal{B},2}^2$ for each entry.

In a similar way, the data received from Alice are decoded by Bob, indicated by $\hat{\mathbf{x}}_{\mathcal{B}}^{(2)}$, and Bob denoises the image using the pretrained DnCNN network as $\bar{\mathbf{I}}_{\mathcal{B}}^{(2)}$. Following the same approach as in the first time slot, Bob recovers the image transmitted from Relay using RLNC decoding as follows:

$$\hat{\mathbf{I}}_{\mathcal{B}}^{(2)} = \left(\bar{\mathbf{I}}_{\mathcal{B}}^{(2)} - \mathbf{M}_{\mathcal{R},2} \circ \mathbf{I}_{\mathcal{R}}^{(ref)}\right) \oslash \mathbf{M}_{\mathcal{R},1}. \tag{8}$$

It is worth noticing that the reference image and the RLNC coefficient matrices employed for RLNC encoding at the Relay are shared with Bob to be able to recover the image transmitted from Relay.

Employing an ISR framework, Bob can also obtain the complete size of the original HR image that Alice sent, which is indicated by $\hat{\mathbf{I}}_{\mathcal{B}}^{(HR,2)}$, as

$$\hat{\mathbf{I}}_{\mathcal{B}}^{(HR,2)} = \nabla_{\epsilon}(\hat{\mathbf{I}}_{\mathcal{B}}^{(2)}). \tag{9}$$

Finally, Bob combines the recovered images in both time slots by overlaying $\hat{\mathbf{I}}_{\mathcal{B}}^{(HR,1)}$ in (5) and $\hat{\mathbf{I}}_{\mathcal{B}}^{(HR,2)}$ in (9) to produce a blended image as

$$\hat{\mathbf{I}}_{\mathcal{B}}^{(HR)} = \nu_1 \hat{\mathbf{I}}_{\mathcal{B}}^{(HR,1)} + \nu_2 \hat{\mathbf{I}}_{\mathcal{B}}^{(HR,2)}, \tag{10}$$

where ν_i, $i \in \{1, 2\}$, denotes the fraction of the i-th HR image in the composite image.

4.5. Image Decoding and Estimation at Eve in Both Time Slots

Because of the wireless medium's broadcast nature, Eve may overhear the data packets carried by Alice and Relay in both time slots, despite the fact that they are not intended for them. The first and second time slots' received signals at Eve can be written by

$$\mathbf{r}_{\mathcal{E}}^{(1)} = \mathbf{x}_{\mathcal{A}} + \mathbf{n}_{\mathcal{E}}^{(1)}, \tag{11}$$

$$\mathbf{r}_{\mathcal{E}}^{(2)} = \mathbf{x}_{\mathcal{R}} + \mathbf{n}_{\mathcal{E}}^{(2)}, \tag{12}$$

respectively, where $\mathbf{n}_{\mathcal{E}}^{(i)}$, $i \in \{1, 2\}$, is an AWGN vector at Eve in the i-th time slot with each entry having zero mean and variance of $\sigma_{\mathcal{E},i}^2$.

Eve begins by attempting to decipher the data from Alice and Relay as $\hat{\mathbf{x}}_{\mathcal{E}}^{(1)}$ and $\hat{\mathbf{x}}_{\mathcal{E}}^{(2)}$, respectively. Next, a deep neural network with a pretrained DnCNN network is also employed to denoise both images as $\bar{\mathbf{I}}_{\mathcal{E}}^{(1)}$ and $\bar{\mathbf{I}}_{\mathcal{E}}^{(2)}$.

Eve, on the other hand, is unaware of the reference images, i.e., $\mathbf{I}_{\mathcal{A}}^{(ref)}$ and $\mathbf{I}_{\mathcal{R}}^{(ref)}$, in the image datastore, which are only shared with legitimate users, along with RLNC coefficient matrices, i.e., $\{\mathbf{M}_{\mathcal{A},1}, \mathbf{M}_{\mathcal{A},2}\}$ and $\{\mathbf{M}_{\mathcal{R},1}, \mathbf{M}_{\mathcal{R},2}\}$, which are used at Alice and Relay for concealing the original image. In order to recover the images, Eve makes an estimate of the RLNC coefficient matrices and searches for the reference images in the datastore.

Let $\{\hat{\mathbf{M}}_{\mathcal{A},1}, \hat{\mathbf{M}}_{\mathcal{A},2}\}$ and $\{\hat{\mathbf{M}}_{\mathcal{R},1}, \hat{\mathbf{M}}_{\mathcal{R},2}\}$ denote the estimated RLNC coefficient matrices at Alice and Relay, respectively. The elements in the RLNC coefficient matrices at Alice and Relay can be estimated as follows:

$$\hat{\alpha}^{(1)}_{\mathcal{X},m,n,p} = \alpha^{(1)}_{\mathcal{X},m,n,p} \pm \varepsilon_{\mathcal{X},m,n,p}, \tag{13}$$

$$\hat{\alpha}^{(2)}_{\mathcal{X},m,n,p} = 1 - \hat{\alpha}^{(1)}_{\mathcal{X},m,n,p}, \tag{14}$$

where $\mathcal{X} \in \{\mathcal{A}, \mathcal{R}\}$, $m \in \{1, 2, \ldots, M'\}$, $n \in \{1, 2, \ldots, N'\}$, $p \in \{1, 2, 3\}$ and $\varepsilon_{\mathcal{X},m,n,p}$ denotes the estimation error of $\hat{\alpha}^{(1)}_{\mathcal{X},m,n,p}$ at Eve.

Additionally, let $\hat{\mathbf{I}}^{(ref)}_{\mathcal{A}}$ and $\hat{\mathbf{I}}^{(ref)}_{\mathcal{R}}$ denote the reference images predicted at Eve for those used at Alice and Relay, respectively. Eve can attempt to decode the original image in the first and the second time slots, respectively, as

$$\hat{\mathbf{I}}^{(1)}_{\mathcal{E}} = \left(\bar{\mathbf{I}}^{(1)}_{\mathcal{E}} - \hat{\mathbf{M}}_{\mathcal{A},2} \circ \hat{\mathbf{I}}^{(ref)}_{\mathcal{A}}\right) \oslash \hat{\mathbf{M}}_{\mathcal{A},1}, \tag{15}$$

$$\hat{\mathbf{I}}^{(2)}_{\mathcal{E}} = \left(\bar{\mathbf{I}}^{(2)}_{\mathcal{E}} - \hat{\mathbf{M}}_{\mathcal{R},2} \circ \hat{\mathbf{I}}^{(ref)}_{\mathcal{R}}\right) \oslash \hat{\mathbf{M}}_{\mathcal{R},1}. \tag{16}$$

Then, Eve can recover the full size of the HR original image by employing ISR in the i-th time slot, $i \in \{1, 2\}$, as

$$\hat{\mathbf{I}}^{(HR,i)}_{\mathcal{E}} = \nabla_{\epsilon}(\hat{\mathbf{I}}^{(i)}_{\mathcal{B}}). \tag{17}$$

The recovered images in both time slots are consequently mixed at Eve in a similar fashion:

$$\hat{\mathbf{I}}^{(HR)}_{\mathcal{E}} = \hat{v}_1 \hat{\mathbf{I}}^{(HR,1)}_{\mathcal{E}} + \hat{v}_2 \hat{\mathbf{I}}^{(HR,2)}_{\mathcal{E}}, \tag{18}$$

where $\hat{v}_i$, $i \in \{1, 2\}$, represents the estimated fraction of the i-th HR image in the composite image at Eve.

For clarity, the above steps of our proposed SCR protocol for image communications in a WRN are illustrated in Figure 2 where there exist a legitimate direct Alice–Bob and relaying Alice–Relay–Bob links along with eavesdropping Alice–Eve and Relay–Eve links.

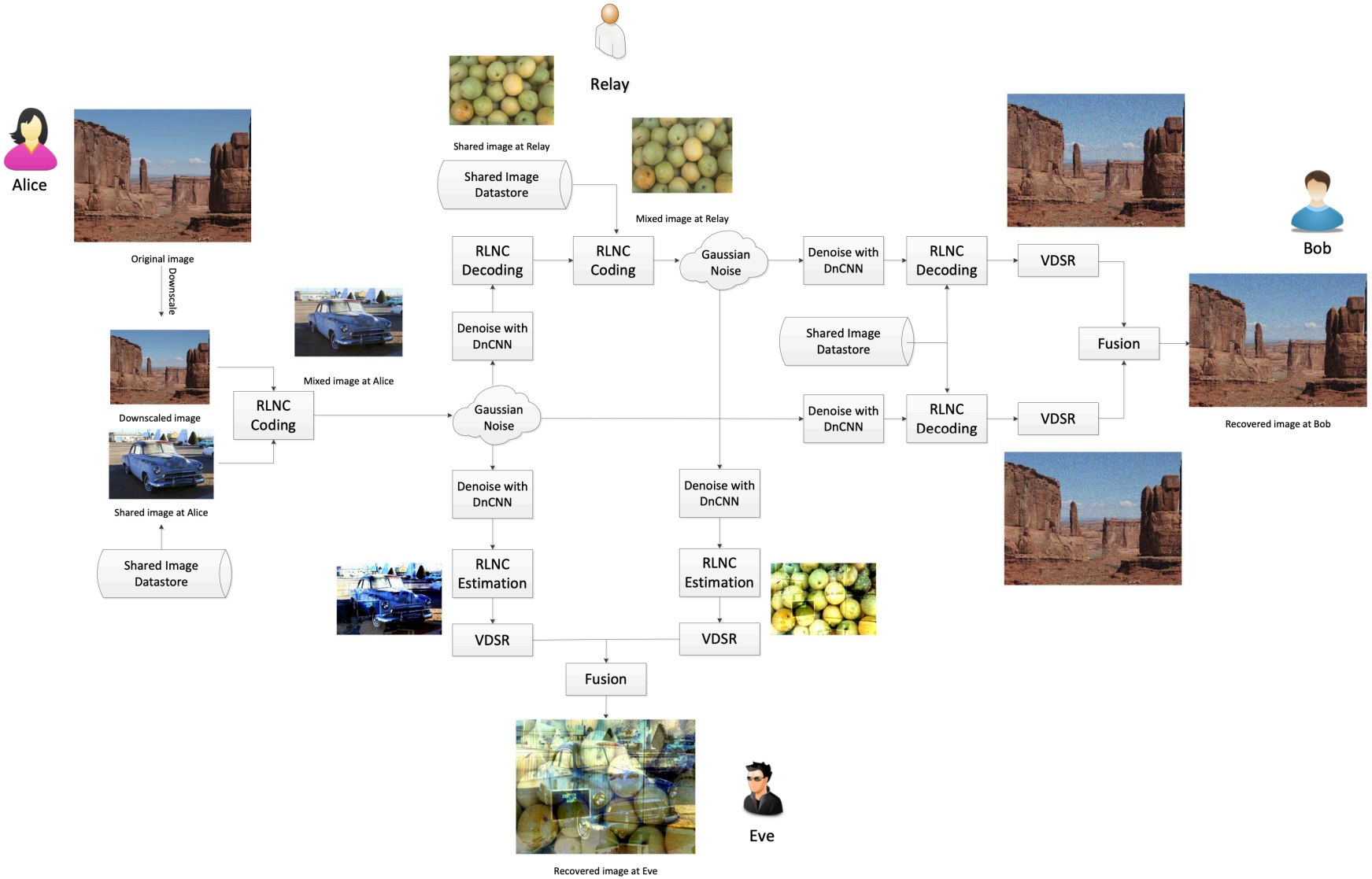

Figure 2. Proposed secure cooperative relaying for image communications with super-resolution.

5. Simulation Results

We provide the simulation results of the proposed SCR protocol for secure image communications across AWGN channels in WRNs in this section. Peak signal-to-noise ratio (PSNR) and structural similarity index measure (SSIM) are two performance metrics used to evaluate the achievement of the proposed approach. (Other security analyses based on information-theoretic has been employed in [43] to analyze the amount of leaked information based on the mutual information between the information sent by Alice and that received by Eve.) The PSNR is used to measure the quality of the recovered image at Bob, i.e., $\hat{\mathbf{I}}_{\mathcal{B}}^{(HR)}$, with respect to the original HR image at Alice, i.e., $\mathbf{I}_{\mathcal{A}}^{(HR)}$, while the SSIM measures the similarity of $\hat{\mathbf{I}}_{\mathcal{B}}^{(HR)}$ and $\mathbf{I}_{\mathcal{A}}^{(HR)}$ based on their visible structure.

Specifically, the PSNR, in decibels (dB), is defined as

$$\begin{aligned} \text{PSNR} &\overset{(a)}{=} 10\log_{10}\frac{1}{\text{MSE}} \\ &\overset{(b)}{=} 10\log_{10}\frac{3MN}{\sum_{x=1}^{M}\sum_{y=1}^{N}\sum_{z=1}^{3}\left(I_A(x,y,z)-\hat{I}_B(x,y,z)\right)^2}, \end{aligned} \tag{19}$$

where MSE in (a) denotes the mean square error between $\hat{\mathbf{I}}_{\mathcal{B}}^{(HR)}$ and $\mathbf{I}_{\mathcal{A}}^{(HR)}$, and (b) is due to the fact that RGB color images are considered of size $M \times N$. The PSNR of the reconstructed image at Eve over wiretap links is also evaluated using (19).

The restored image's average SSIM at Bob i.e., $\hat{\mathbf{I}}_{\mathcal{B}}^{(HR)}$, is computed by [44]

$$\text{SSIM} = \frac{1}{MN}\sum_{x=1}^{M}\sum_{y=1}^{N}[l_{\mathcal{A},\mathcal{B}}(x,y)]^{\alpha}[c_{\mathcal{A},\mathcal{B}}(x,y)]^{\beta}[s_{\mathcal{A},\mathcal{B}}(x,y)]^{\gamma}, \tag{20}$$

where $l_{\mathcal{A},\mathcal{B}}(x,y)$, $c_{\mathcal{A},\mathcal{B}}(x,y)$ and $s_{\mathcal{A},\mathcal{B}}(x,y)$ represent the luminance, contrast and structure components, respectively, at pixel (x,y). Here, α, β and γ refer to the weighted combination of these three components correspondingly.

In the following, the performance of the SCR protocol is first compared to that of the SDT protocol, which utilizes just a direct Alice–Bob link, and the SRT protocol, which has only relaying Alice–Relay–Bob links. The impacts of the reference image estimated at Eve, the shared image database between legitimate users, the legitimate communication links, and the wiretap links are then evaluated sequentially to validate the benefit of the proposed SCR protocol in enhancing the security of image communications with the assistance of the relay. For both training and validation, the simulation is carried out in MATLAB. The ISR is trained using an image dataset from the IAPR TC-12 benchmark [42], which consists of 20,000 still natural images. The scaling factor is in the range 2, 4, 6, 8, 10, the image patch size is 41 by 41, the number of patches per image is 64, and the number of convolutional layers is 20. Specifically, the image input layer consists of 64 3-by-3 filters; the middle layers are made up of 18 alternating convolutional and rectified linear unit (ReLU) layers; the penultimate layer is a convolutional layer with a single 3-by-3-by-64 filter; and the final layer is a regression layer instead of a ReLU layer to compute the MSE between the residual image and network prediction. The ISR network is trained with stochastic gradient descent and momentum optimization using the following hyper-parameter settings: the learning rate is initially set at 0.1 and is reduced by a factor of 10 every 10 epochs up to a maximum of 100 epochs; momentum is set to 0.9; and gradient clipping is enabled using the L2-norm approach to clip gradient values with a gradient threshold of 0.01. For the validation step, 20 undistorted images in Figure 3 from the Image Processing Toolbox in MATLAB are used. It is worth noting that our research is the first approach employing the SCR with RLNC and ISR for secure image communications in WRNs.

Figure 3. Images for testing and validation of the proposed cooperative secure image super-resolution.

5.1. SCR Protocol versus SRT versus SDT Protocols

Evaluating the effectiveness of the proposed SCR protocol, Figure 4 illustrates the PSNR and SSIM as a function of the noise variance of the direct Alice–Bob link in the first time slot, i.e., $\sigma^2_{\mathcal{B},1}$. Three secure image communication protocols, including SDT, SRT and the proposed SCR, are considered for comparison. It is assumed that Relay is located between Alice and Bob, where the relaying Alice–Relay and Relay–Bob links experience the same noise variance, which is equal to half of the noise variance of the direct Alice–Bob link, i.e., $\sigma^2_{\mathcal{R},1} = \sigma^2_{\mathcal{B},2} = \sigma^2_{\mathcal{B},1}/2$. The noise variances of the wiretap Alice–Eve and Relay–Eve links are assumed to be the same as those of Alice–Bob and Relay–Bob links, respectively, i.e., $\sigma^2_{\mathcal{E},1} = \sigma^2_{\mathcal{R},1}$ and $\sigma^2_{\mathcal{E},2} = \sigma^2_{\mathcal{B},2}$. The original HR images at Alice are first downscaled by four times, i.e., $\epsilon = 4$, prior to transmission. For encoding at Alice and Relay, the elements in RLNC matrices are supposed to be in the range $[0.3, 0.5]$ and known to Bob. For comparison of different secure image communication protocols, in this subsection, Eve is assumed to be aware of the reference images used for the RLNC encoding. As shown in Figure 4a,b, all protocols gain a greater PSNR performance at Bob up to 8 dB in the PSNR than that at Eve since Eve does not know the RLNC coefficient matrices used at Alice and Bob. In particular, the SCR protocol, for example, outperforms both the SRT and SDT protocols by 0.5 dB and 2 dB, respectively. This is due to the fact that, in the SCR protocol, Relay assists the image communications via relaying links along with the direct link between Alice and Bob, while there is only a direct Alice–Bob link in the SDT protocol and only relaying Alice–Relay and Relay–Bob links are available in the SRT protocol.

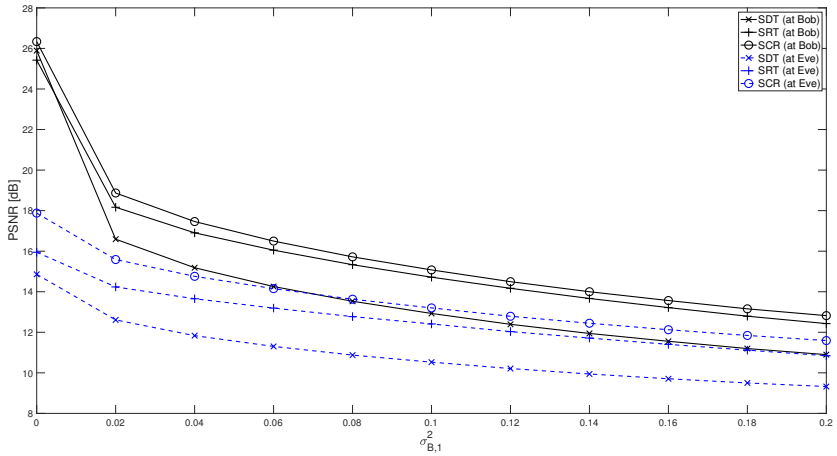

(**a**) PSNR versus noise variance of Alice–Bob link.

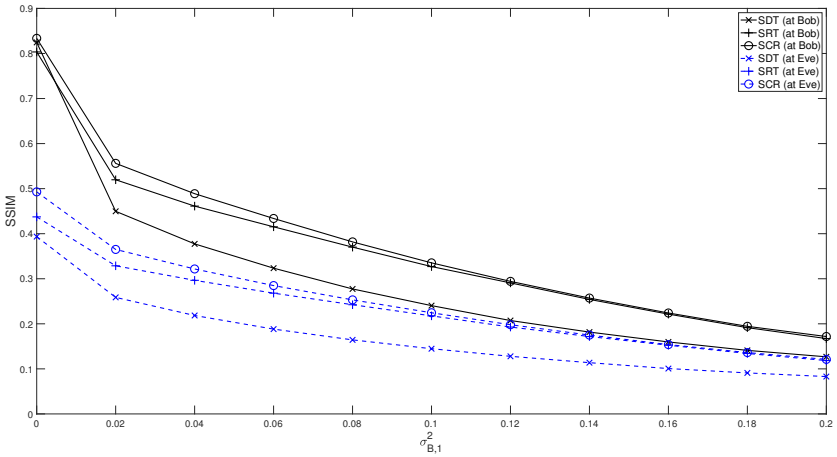

(**b**) SSIM versus noise variance of Alice–Bob link.

Figure 4. PSNR and SSIM of secure image communication protocols.

5.2. Effectiveness of SCR Protocol for Secure Image Communications

The effectiveness of the proposed SCR protocol is further illustrated in Figure 5 where the PSNR and SSIM of different secure image communication protocols are plotted versus the noise variance $\sigma^2_{\mathcal{B},1}$ of the direct Alice–Bob link when the reference images are incorrectly estimated at Eve, i.e., $\hat{\mathbf{I}}^{(ref)}_{\mathcal{A}}$ and $\hat{\mathbf{I}}^{(ref)}_{\mathcal{R}}$. Specifically, Eve uses the 9th reference image (see Figure 3) to decode the image received in both the first and the second time slots, while the correct reference images at Alice and Relay are the 20th and 11th images, respectively. Three protocols, including SDT, SRT and the proposed SCR, are also considered with the same simulation settings as in Figure 4. It can be perceived in Figure 5a,b that a significantly enhanced performance is attained at Bob compared to Eve due to the incorrect reference image estimated at Eve. Specifically, the PSNR at Bob in the SCR protocol is of up to 16 dB higher than that at Eve. Furthermore, the SCR protocol with Relay collaboration has been demonstrated to perform better than both the SRT and SDT protocols. This validates the SCR protocol's usefulness in providing secure image communications between Alice and Bob in WRNs.

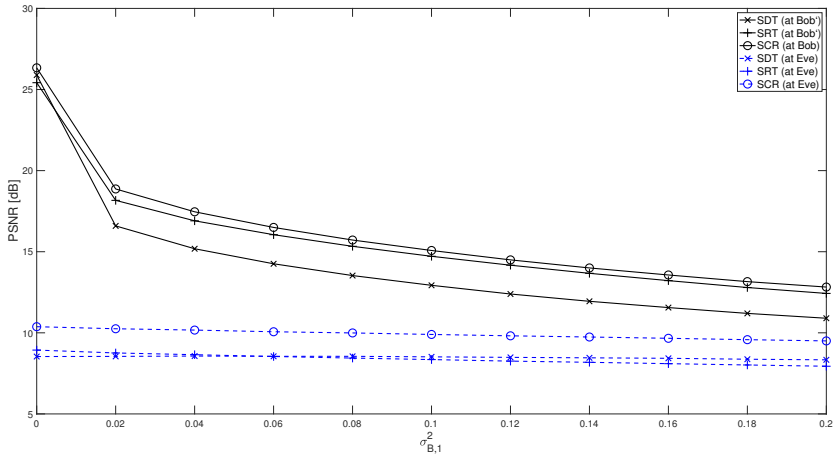

(**a**) PSNR versus $\sigma^2_{\mathcal{B},1}$ with incorrect $\hat{\mathbf{I}}^{(ref)}_{\mathcal{A}}$ and $\hat{\mathbf{I}}^{(ref)}_{\mathcal{R}}$.

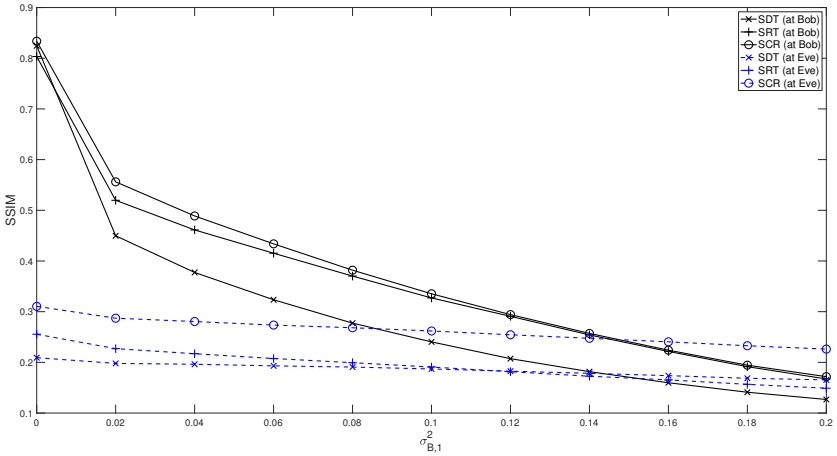

(**b**) SSIM versus $\sigma^2_{\mathcal{B},1}$ with incorrect $\hat{\mathbf{I}}^{(ref)}_{\mathcal{A}}$ and $\hat{\mathbf{I}}^{(ref)}_{\mathcal{R}}$.

Figure 5. PSNR and SSIM of secure image communication protocols with reference images incorrectly estimated at Eve.

5.3. Impacts of Shared Image Dataset

The effects of the reference images are emphasized in Figure 6, where the PSNR and SSIM are drawn against the noise variance $\sigma^2_{\mathcal{B},1}$ of the direct link between Alice and Bob with various reference images $\hat{\mathbf{I}}^{(ref)}_{\mathcal{A}}$ and $\hat{\mathbf{I}}^{(ref)}_{\mathcal{R}}$ chosen at Eve. When Eve decodes the overheard images from Alice and Relay for the first and second time slots, respectively, using various reference images, including the 9th, 10th, 14th and 15th images (see Figure 3), the performance of the SCR protocol is assessed using the same simulation parameters as in Figure 5. As seen in Figure 6a,b, the incorrect reference image has a significant negative impact on Eve's performance. For instance, the best PSNR that Eve can achieve with the 14th reference image over noise-free channels is 15 dB lower than that at Bob and the performance at Eve is even worse when other wrong reference images are used for decoding. Another reason for this degraded performance is that Eve does not know the RLNC coefficient matrices at Alice and Relay. This again shows the effectiveness of the proposed SCR protocol for secure image communications in WRNs.

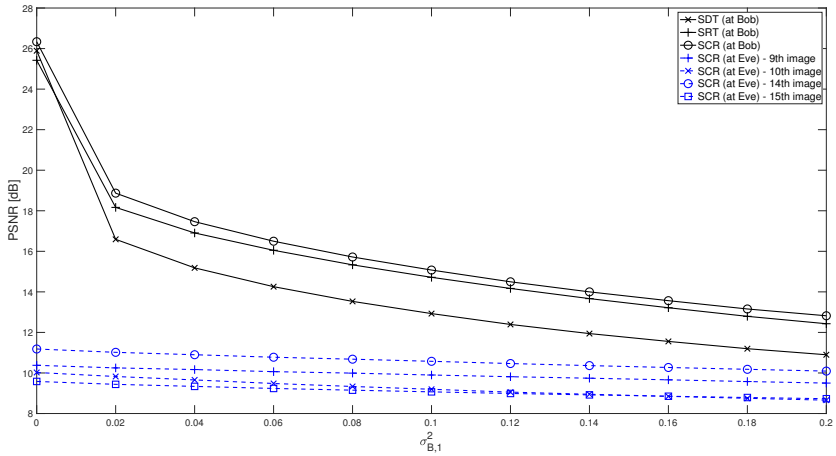

(**a**) PSNR versus $\sigma^2_{\mathcal{B},1}$ with different $\hat{\mathbf{I}}^{(ref)}_{\mathcal{A}}$ and $\hat{\mathbf{I}}^{(ref)}_{\mathcal{R}}$.

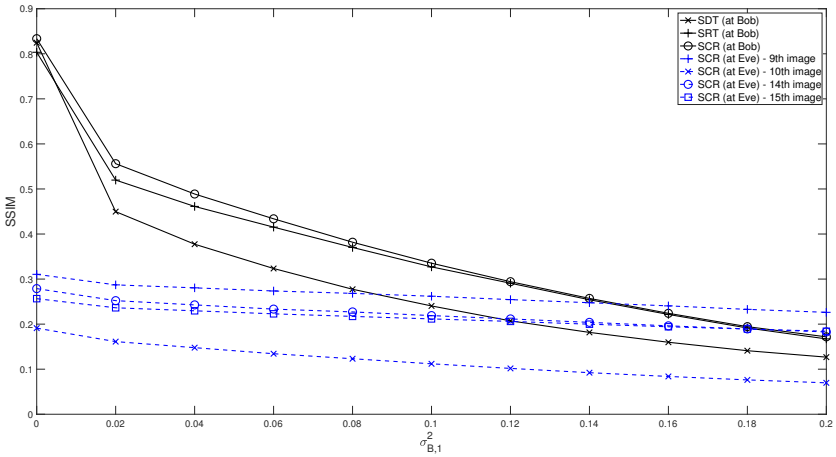

(**b**) SSIM versus $\sigma^2_{\mathcal{B},1}$ with different $\hat{\mathbf{I}}^{(ref)}_{\mathcal{A}}$ and $\hat{\mathbf{I}}^{(ref)}_{\mathcal{R}}$.

Figure 6. PSNR and SSIM versus noise variance of Alice–Bob link with respect to different reference images incorrectly estimated at Eve.

5.4. Impacts of Scaling Factor

In order to investigate the impacts of scaling factors on the performance of secure image communications in WRNs, Figure 7 plots the PSNR and SSIM of the proposed SCR protocol versus the noise variance $\sigma^2_{\mathcal{B},1}$ of the direct link connecting Alice and Bob in the first time slot with regard to various scaling factors, i.e., $\epsilon = 4, 6, 8, 10$. Eve uses the wrong reference image for decoding and the same simulation parameters as in Figure 5 are taken into account. The PSNR and SSIM at Bob fall as the scale grows in a low-noise environment, as shown in Figure 7a,b, although this has little impact in a high-noise environment. In particular, when ϵ is changed from 4 to 10, the PSNR at Bob is reduced by up to 4 dB as $\sigma^2_{\mathcal{B},1} < 0.04$ and by less than 1 dB as $\sigma^2_{\mathcal{B},1} > 0.14$. This illustrates how well the proposed approach works to reduce transmission bandwidth by raising the scaling factor with just a minimal impact on the quality of the recovered image, particularly in noisy environments. Additionally, this adjustment in the scale factor's lowering has little impact on Eve's performance. This is because, regardless of the scaling factor, Eve cannot decode the image without knowledge of the RLNC coefficient matrices and reference images used at Alice and Relay for encoding.

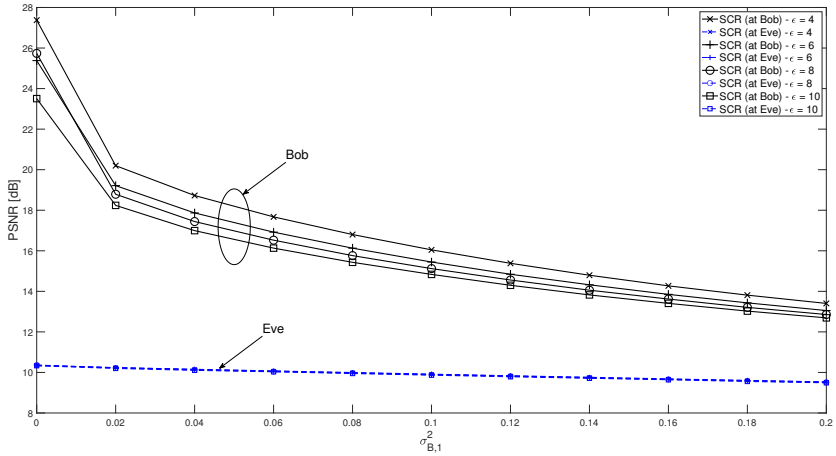

(**a**) PSNR versus $\sigma^2_{\mathcal{B},1}$ with different ϵ.

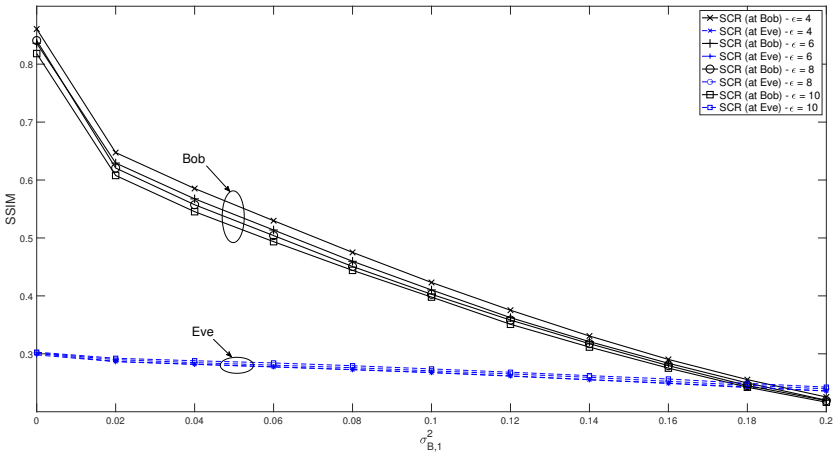

(**b**) SSIM versus $\sigma^2_{\mathcal{B},1}$ with different ϵ.

Figure 7. PSNR and SSIM versus noise variance of Alice–Bob link with respect to different scaling factors.

5.5. Impacts of Direct Link on Secure Image Communications

Taking into account the direct link in WRNs, Figure 8 plots the PSNR and SSIM of various secure image communication protocols as functions of the noise variance of Alice–Bob link, i.e., $\sigma^2_{\mathcal{B},1}$. The noise variances of Alice–Relay, Relay–Bob, Alice–Eve and Relay–Eve links are fixed as $\sigma^2_{\mathcal{R},1} = \sigma^2_{\mathcal{B},2} = 0.1$, $\sigma^2_{\mathcal{E},1} = 0.2$ and $\sigma^2_{\mathcal{E},2} = 0.1$, respectively. Three secure image communication protocols, i.e., SDT, SRT and the proposed SCR, are also considered with the same assumption that the original HR images at Alice are firstly downscaled with a scaling factor $\epsilon = 4$ prior to transmission and the elements in RLNC matrices for encoding at Alice and Relay are in the range $[0.3, 0.5]$, which are known to Bob. It can be observed in Figure 8a,b that the proposed SCR protocol achieves a better performance at Bob than the SRT protocol for the whole range of $\sigma^2_{\mathcal{B},1}$ and it is shown to be better than the SDT protocol at high $\sigma^2_{\mathcal{B},1}$. The SDT protocol is, however, better than both the SCR and SRT protocols at low $\sigma^2_{\mathcal{B},1}$. This reflects the practical scenario in which Relay is efficient when the direct Alice–Bob link suffers from high noise. In other words, the usage of Relay is not always necessary, especially when the direct Alice–Bob link is already of good quality.

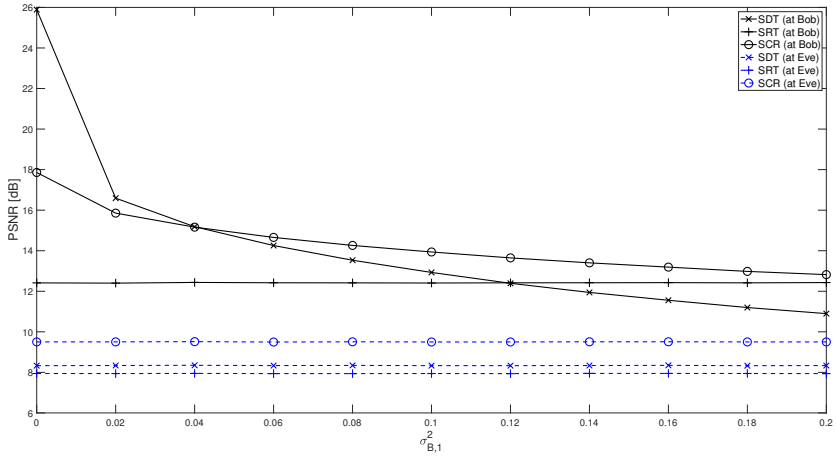

(**a**) PSNR versus $\sigma^2_{\mathcal{B},1}$.

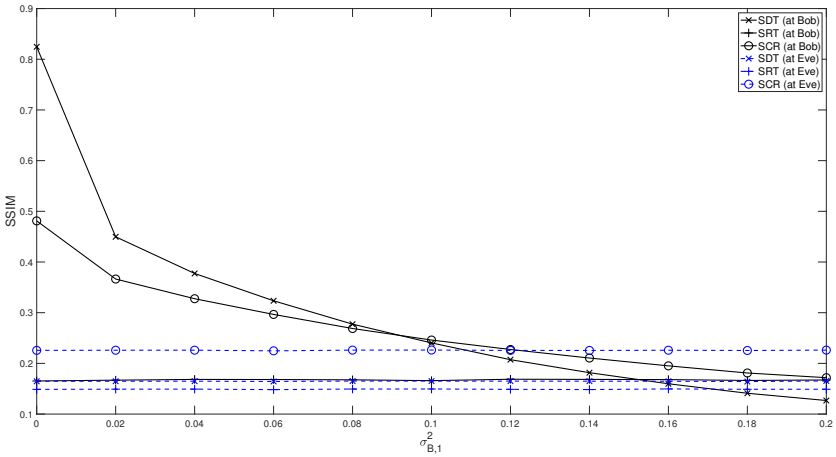

(**b**) SSIM versus $\sigma^2_{\mathcal{B},1}$.

Figure 8. PSNR and SSIM versus noise variance of Alice–Bob link.

5.6. Impacts of Relaying Links on Secure Image Communications

Both relaying links, i.e., Alice–Relay and Relay–Bob links, are crucial to enhance the performance of the image transmission from Alice to Bob with the assistance of Relay in WRNs. Figure 9 plots the PSNR and SSIM of different protocols versus the noise variance of Alice–Relay link, i.e., $\sigma^2_{\mathcal{R},1}$, while the impacts of Relay–Bob link, i.e., $\sigma^2_{\mathcal{B},2}$, on the performance of the secure image communications are illustrated in Figure 10. It is assumed that the noise variance of Relay–Bob link is $\sigma^2_{\mathcal{B},2} = 0.1$ in Figure 9, while that of Alice–Relay link is $\sigma^2_{\mathcal{R},1} = 0.1$ dB in Figure 10. In both figures, the noise variances of other links are $\sigma^2_{\mathcal{B},1} = 0.2$, $\sigma^2_{\mathcal{E},1} = 0.2$ and $\sigma^2_{\mathcal{E},2} = 0.1$, whereas other parameters are similarly set as those in Figure 8. It can be observed in Figures 9 and 10 that a better performance is achieved with the proposed SCR protocol compared to the SRT protocol at high $\sigma^2_{\mathcal{R},1}$ and high $\sigma^2_{\mathcal{B},2}$. Meanwhile, the SDT scheme is shown to be independent of the quality of the relaying links as Relay is not involved in communications between Alice and Bob. Specifically, an enhancement of 1 dB and 2 dB in PSNR can be achieved with the SCR protocol compared to the SRT protocol when $\sigma^2_{\mathcal{R},1} = 0.2$ and $\sigma^2_{\mathcal{B},2} = 0.2$, respectively. This is due to the fact that the direct link can collaborate with the relaying links to decode the image at Bob in the SCR protocol when the relaying links suffer from high noise.

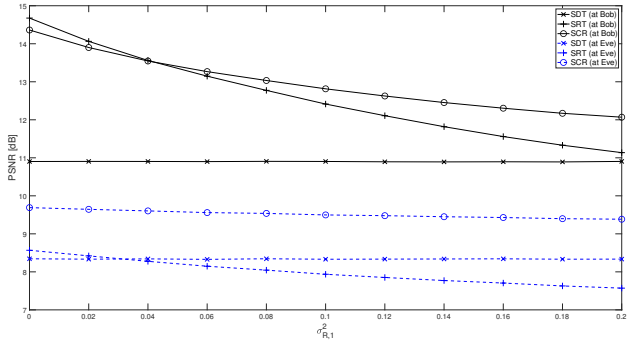

(**a**) PSNR versus $\sigma^2_{\mathcal{R},1}$.

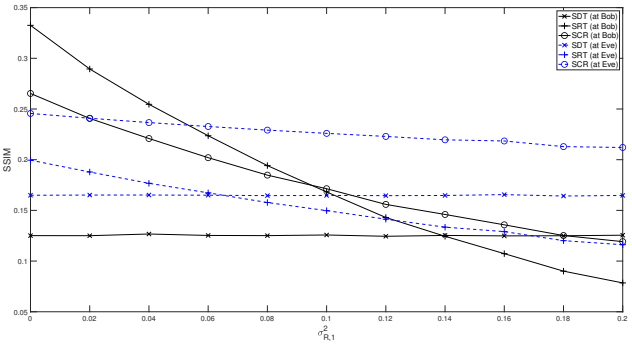

(**b**) SSIM versus $\sigma^2_{\mathcal{R},1}$.

Figure 9. PSNR and SSIM versus noise variance of Alice–Relay link.

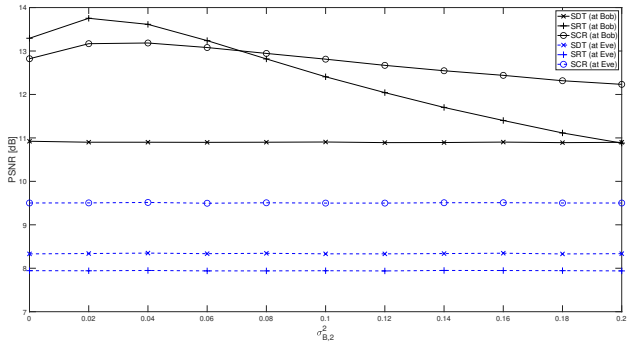

(**a**) PSNR versus $\sigma^2_{\mathcal{B},2}$.

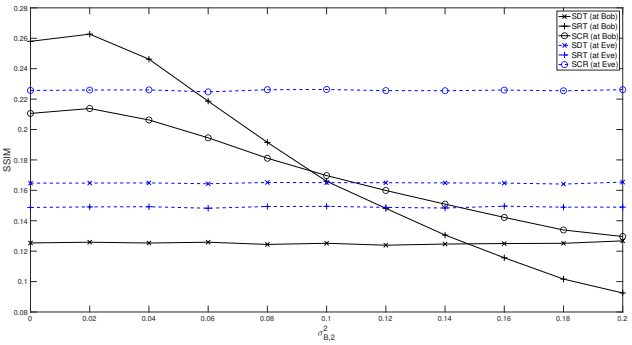

(**b**) SSIM versus $\sigma^2_{\mathcal{B},2}$.

Figure 10. PSNR and SSIM versus noise variance of Relay–Bob link.

5.7. Impacts of Wiretap Links on Secure Image Communications

Considering the scenario when Eve may experience different wiretap channels, Figures 11 and 12 sequentially plot the PSNR and SSIM of different secure image protocols against the noise variances of the Alice–Eve link and Relay–Eve link, respectively. In both figures, the noise variances of Alice–Bob, Alice–Relay and Relay–Bob links are set as $\sigma^2_{\mathcal{B},1} = 0.2$, $\sigma^2_{\mathcal{R},1} = 0.1$ and $\sigma^2_{\mathcal{B},2} = 0.1$, respectively. For wiretap channels, the noise variance of the Relay–Eve link is $\sigma^2_{\mathcal{E},2} = 0.1$, while the Alice–Eve link in Figure 12 experiences a noise with $\sigma^2_{\mathcal{E},1} = 0.2$. It can be seen in both Figures 11 and 12 that the performance at Eve is not much affected by the variation in noise variances of the wiretap links. Specifically, the PSNR at Eve with the SCR protocol reduces 0.5 dB and 0.2 dB when $\sigma^2_{\mathcal{E},1}$ and $\sigma^2_{\mathcal{E},2}$ increase from 0 to 0.2, while there is only a slight change in the performance of the SRT and SDT protocols. In fact, Eve is not aware of the RLNC coefficient matrices nor the reference images used at Alice and Relay; consequently, an enhanced quality of wiretap links does not help improve the decoding performance at Eve.

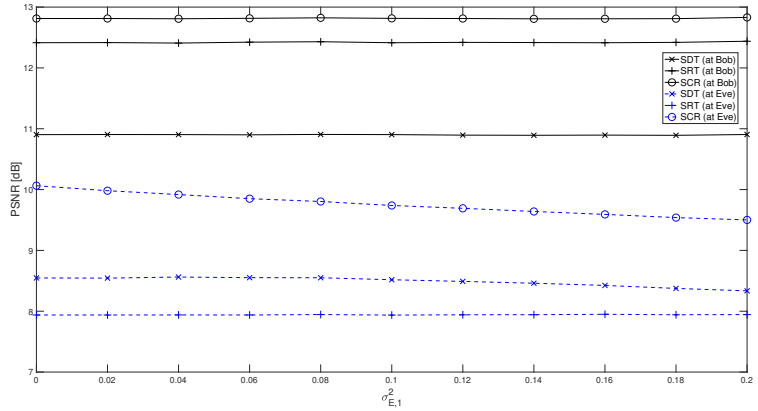

(**a**) PSNR versus $\sigma^2_{\mathcal{E},1}$.

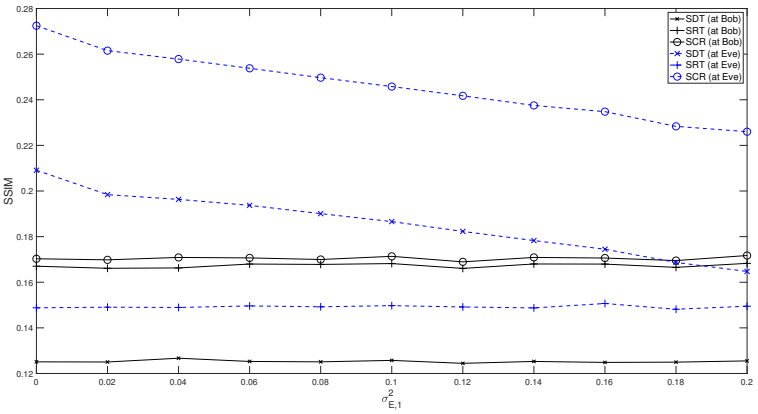

(**b**) SSIM versus $\sigma^2_{\mathcal{E},1}$.

Figure 11. PSNR and SSIM versus noise variance of Alice–Eve link.

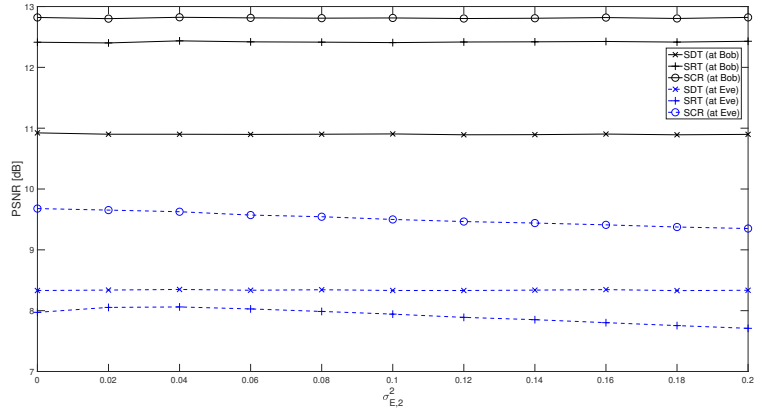

(**a**) PSNR versus $\sigma^2_{\mathcal{E},2}$.

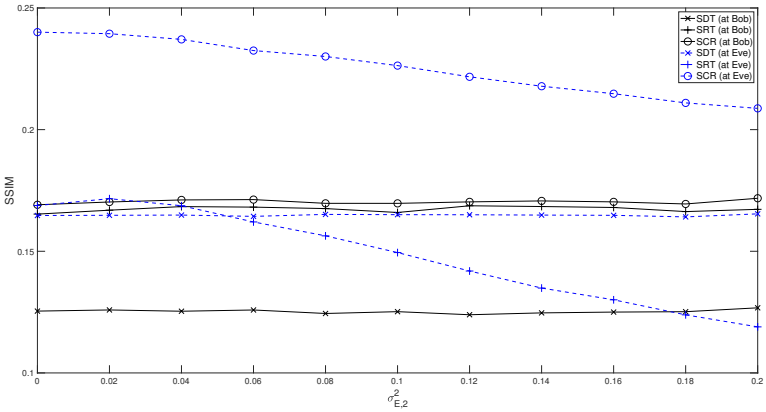

(**b**) SSIM versus $\sigma^2_{\mathcal{E},2}$.

Figure 12. PSNR and SSIM versus noise variance of Relay–Eve link.

6. Conclusions

In this paper, we have proposed an SCR protocol for image communications in WRNs where Alice wishes to securely transfer HR images to Bob with the assistance of Relay via two hops. RLNC has been employed at Alice and Relay to conceal the original image from Eve. Also, ISR has been applied to recover the HR images at Bob from their LR versions which were downscaled at Alice prior to transmitting to Relay and Bob. It has been shown that the proposed SCR protocol achieves a much higher PSNR at Bob of up to 16 dB compared to that at Eve. Exploiting both direct and relaying links, the SCR protocol attains an enhancement of 0.5 dB and 2 dB over the SRT and SDT protocols, respectively. Furthermore, the SCR protocol allows the original HR images to be downscaled to LR images of up to ten times to save the transmission bandwidth prior to sending to Bob and Relay, but there is only a slight change in the image quality with less than 1 dB in the noisy environment. Investigating the impacts of communication links in the WRNs, it has been demonstrated that Relay is only necessary when the direct Alice–Bob link experiences high noise and relaying links are critical in the SCR protocols to enhance the decoding performability at Bob by collaborating with the direct link. In particular, given lack of knowledge of RLNC coefficient matrices used at Alice and Relay along with reference images in the shared image datastore, Eve can not decode the original HR images, even with high-quality wiretap links and ISR. This accordingly verifies and confirms the efficiency of the proposed SCR protocol in securing the transmission of the original HR images with a limited transmission bandwidth in the WRNs. Future research will delve into integrating encryption into the RLNC along with DL-based aggregation and signature

in multiple-relay networks over fading channels to improve the security and robustness of the SCR protocol.

Author Contributions: Conceptualization, H.-T.D. and Q.-T.V.; Methodology, H.-T.D.; Software, H.-T.D. and Q.-T.V.; Investigation, H.-T.D. and T.T.N.; Validation, H.-T.D. and T.T.N.; Formal analysis, H.-T.D.; Writing—origianl draft, H.-T.D.; Writing—review & editing, H.-T.D., C.V.P. and Q.-T.V.; Supervision, C.V.P. and Q.-T.V. All authors have read and agreed to the published version of the manuscript.

Funding: This study was self-funded by the authors.

Data Availability Statement: The data presented in this study are available on request from the corresponding author. The data are not publicly available due to their use for further research.

Conflicts of Interest: The authors declare no conflict of interest.

References

1. Sendonaris, A.; Erkip, E.; Aazhang, B. User cooperation diversity. Part I. System description. *IEEE Trans. Commun.* **2003**, *51*, 1927–1938. [CrossRef]
2. Nosratinia, A.; Hunter, T.; Hedayat, A. Cooperative communication in wireless networks. *IEEE Commun. Mag.* **2004**, *42*, 74–80. [CrossRef]
3. Ahlswede, R.; Cai, N.; Li, S.-Y.; Yeung, R. Network information flow. *IEEE Trans. Inf. Theory* **2000**, *46*, 1204–1216. [CrossRef]
4. Louie, R.; Li, Y.; Vucetic, B. Practical physical layer network coding for two-way relay channels: Performance analysis and comparison. *IEEE Trans. Wirel. Commun.* **2010**, *9*, 764–777. [CrossRef]
5. Vien, Q.-T.; Le, T.A.; Nguyen, H.X.; Le-Ngoc, T. A physical layer network coding based modify-and-forward with opportunistic secure cooperative transmission protocol. *Mob. Netw. Appl.* **2019**, *24*, 464–479. [CrossRef]
6. Koetter, R.; Medard, M. An algebraic approach to network coding. *IEEE/ACM Trans. Netw.* **2003**, *11*, 782–795. [CrossRef]
7. Ju, M.; Kim, I.-M. Error performance analysis of BPSK modulation in physical-layer network-coded bidirectional relay networks. *IEEE Trans. Commun.* **2010**, *58*, 2770–2775. [CrossRef]
8. Nguyen, D.; Tran, T.; Nguyen, T.; Bose, B. Wireless broadcast using network coding. *IEEE Trans. Veh. Technol.* **2009**, *58*, 914–925. [CrossRef]
9. Soljanin, E. Network multicast with network coding [lecture notes]. *IEEE Signal Process. Mag.* **2008**, *25*, 109–112. [CrossRef]
10. Lima, L.; Médard, M.; Barros, J. Random linear network coding: A free cipher? In Proceedings of the 2007 IEEE International Symposium On Information Theory, Nice, France, 24–29 June 2007; pp. 546–550.
11. Wang, Z.; Chen, J.; Hoi, S.C. Deep learning for image super-resolution: A survey. *IEEE Trans. Pattern Anal. Mach. Intell.* **2020**, *43*, 3365–3387. [CrossRef]
12. Vien, Q.-T.; Nguyen, T.T.; Nguyen, H.X. Deep-NC: A secure image transmission using deep learning and network coding. *Signal Process. Image Commun.* **2021**, *99*, 116490. [CrossRef]
13. Ooi, Y.K.; Ibrahim, H. Deep learning algorithms for single image super-resolution: A systematic review. *Electronics* **2021**, *10*, 7. [CrossRef]
14. Yang, W.; Zhang, X.; Tian, Y.; Wang, W.; Xue, J.; Liao, Q. Deep Learning for Single Image Super-Resolution: A Brief Review. *IEEE Trans. Multimed.* **2019**, *21*, 3106–3121. [CrossRef]
15. Dong, C.; Loy, C.C.; He, K.; Tang, X. Learning a deep convolutional network for image super-resolution. In *Computer Vision—ECCV 2014*; Fleet, D., Pajdla, T., Schiele, B., Tuytelaars, T., Eds.; Springer International Publishing: Cham, Switerland, 2014; pp. 184–199.
16. Lai, W.; Huang, J.; Ahuja, N.; Yang, M. Deep laplacian pyramid networks for fast and accurate super-resolution. In Proceedings of the 2017 IEEE Conference on Computer Vision and Pattern Recognition (CVPR), Honolulu, HI, USA, 21–26 July 2017; pp. 5835–5843.
17. Haris, M.; Shakhnarovich, G.; Ukita, N. Deep back-projection networks for super-resolution. In Proceedings of the 2018 IEEE/CVF Conference on Computer Vision and Pattern Recognition, Salt Lake City, UT, USA, 18–23 June 2018; pp. 1664–1673.
18. Li, Z.; Yang, J.; Liu, Z.; Yang, X.; Jeon, G.; Wu, W. Feedback network for image super-resolution. In Proceedings of the IEEE/CVF Conference on Computer Vision and Pattern Recognition (CVPR), Long Beach, CA, USA, 15–20 June 2019; pp. 3867–3876.
19. Kim, J.; Lee, J.K.; Lee, K.M. Accurate image super-resolution using very deep convolutional networks. In Proceedings of the IEEE Conference on Computer Vision and Pattern Recognition, Las Vegas, NV, USA, 27–30 June 2016; pp. 1646–1654.
20. Kim, J.; Lee, J. Deep Residual Network With Enhanced Upscaling Module for Super-Resolution. In Proceedings of the IEEE Conference On Computer Vision And Pattern Recognition (CVPR) Workshops, Salt Lake City, UT, USA, 18–23 June 2018; pp. 913–921.
21. Pan, J.; Ye, N.; Yu, H.; Hong, T.; Al-Rubaye, S.; Mumtaz, S.; Al-Dulaimi, A.; Chih-Lin, I. AI-driven blind signature classification for IoT connectivity: A deep learning approach. *IEEE Trans. Wirel. Commun.* **2022**, *21*, 6033–6047. [CrossRef]
22. Rahim, T.; Khan, S.; Usman, M.A.; Shin, S.Y. Exploiting de-noising convolutional neural networks dncnns for an efficient watermarking scheme: A case for information retrieval. *IETE Tech. Rev.* **2020**, *38*, 245–255 . [CrossRef]

23. Zhao, Y.; Li, Y.; Dong, X.; Yang, B. Low-frequency noise suppression method based on improved dncnn in desert seismic data. *IEEE Geosci. Remote Sens. Lett.* **2019**, *16*, 811–815. [CrossRef]
24. Zhang, K.; Zuo, W.; Chen, Y.; Meng, D.; Zhang, L. Beyond a Gaussian denoiser: Residual learning of deep CNN for image denoising. *IEEE Trans. Image Process.* **2017**, *26*, 3142–3155. [CrossRef] [PubMed]
25. Vien, Q.-T.; Tuan, N.T.; Huan, N.X. A lightweight secure image super resolution using network coding.In Proceedings of the International Conference on Computer Vision Theory and Applications (VISAPP 2021), Vienna, Austria, 8–10 February, 2021; pp. 653–660.
26. Guerrini, F.; Dalai, M.; Leonardi, R. Minimal information exchange for secure image hash-based geometric transformations estimation. *IEEE Trans. Inf. Forensics Secur.* **2020**, *15*, 3482–3496. [CrossRef]
27. Kaur, M.; Kumar, V. A comprehensive review on image encryption techniques. *Arch. Comput. Methods Eng.* **2020**, *27*, 15–43. [CrossRef]
28. Peng, H.; Yang, B.; Li, L.; Yang, Y. Secure and traceable image transmission scheme based on semitensor product compressed sensing in telemedicine system. *IEEE Internet Things J.* **2020**, *7*, 2432–2451. [CrossRef]
29. Chan, C.; Cheng, L. Hiding data in images by simple LSB substitution. *Pattern Recognit.* **2004**, *37*, 469–474. [CrossRef]
30. Bender, W.; Gruhl, D.; Morimoto, N.; Lu, A. Techniques for data hiding. *IBM Syst. J.* **1996**, *35*, 313–336. [CrossRef]
31. Franz, E.; Jerichow, A.; Möller, S.; Pfitzmann, A.; Stierand, I. Computer based steganography: How it works and why therefore any restrictions on cryptography are nonsense, at best. In *Information Hiding*; Anderson, R., Ed.; Springer Berlin/Heidelberg, Germany, 1996; pp. 7–21.
32. Hashad, A.I.; Madani, A.S.; Wahdan, A.E.M.A. A robust steganography technique using discrete cosine transform insertion. In Proceedings of the 2005 International Conference on Information and Communication Technology, Cairo, Egypt, 5–6 December 2005, pp. 255–264.
33. Chen, P.-Y.; Lin, H.-J. A DWT based approach for image steganography. *Int. J. Appl. Sci. Eng.* **2006**, *4*, 275–290.
34. Qin, J.; Luo, Y.; Xiang, X.; Tan, Y.; Huang, H. Coverless image steganography: A survey. *IEEE Access* **2019**, *7*, 171372–171394. [CrossRef]
35. Zhang, S.; Liew, S.C.; Lam, P.P. Hot topic: Physical-layer network coding. In Proceedings of the ACM MobiCom'06, Los Angeles, CA, USA, 23–29 September 2006; pp. 358–365.
36. Vien, Q.-T.; Nguyen, H.X.; Stewart, B.G.; Choi, J.; Tu, W. On the energy-delay tradeoff and relay positioning of wireless butterfly networks. *IEEE Trans. Veh. Technol.* **2015**, *64*, 159–172. [CrossRef]
37. Cai, N.; Yeung, R. Secure network coding. In Proceedings of the IEEE International Symposium on Information Theory, Lausanne, Switzerland, 30 June–5 July 2002; p. 323.
38. Cui, T.; Ho, T.; Kliewer, J. On secure network coding with nonuniform or restricted wiretap sets. *IEEE Trans. Inf. Theory* **2013**, *59*, 166–176. [CrossRef]
39. Khan, A.; Chatzigeorgiou, I. Opportunistic relaying and random linear network coding for secure and reliable communication. *IEEE Trans. Wirel. Commun.* **2017**, *17*, 223–234. [CrossRef]
40. Tajbakhsh, S.; Coon, J.; Chen, G. Network coding for physical layer secrecy. *IEEE Wirel. Commun. Lett.* **2018**, *7*, 642–645. [CrossRef]
41. Yu, H.; Shen, Z.; Miao, C.; Leung, C.; Niyato, D. A survey of trust and reputation management systems in wireless communications. *Proc. IEEE* **2010**, *98*, 1755–1772. [CrossRef]
42. Grubinger, M.; Clough, P.D.; Müller, H.; Deselaers, T. The IAPR TC-12 benchmark: A new evaluation resource for visual information systems. In Proceedings of the International Workshop OntoImage'2006 Language Resources for Content-Based Image Retrieval, Held in conjunction with LREC'06, Genoa, Italy, 22 May 2006; pp. 13–23.
43. Cai, N.; Chan, T. Theory of secure network coding. *Proc. IEEE* **2011**, *99*, 421–437.
44. Wang, Z.; Bovik, A.C.; Sheikh, H.R.; Simoncelli, E.P. Image quality assessment: From error visibility to structural similarity. *IEEE Trans. Image Process.* **2004**, *13*, 600–612. [CrossRef] [PubMed]